Electronic density of states of helically-wrapped carbon nanotubes

2007 J. Phys.: Condens. Matter 19 406227

(http://iopscience.iop.org/0953-8984/19/40/406227)

IOP PUBLISHING JOURNAL OF PHYSICS: CONDENSED MATTER

J. Phys.: Condens. Matter **19** (2007) 406227 (10pp) doi:10.1088/0953-8984/19/40/406227

Electronic density of states of helically-wrapped carbon nanotubes

Andrew Wall and Mauro S Ferreira

School of Physics, Trinity College Dublin, Dublin 2, Republic of Ireland

E-mail: ferreirm@tcd.ie

Received 23 May 2007, in final form 30 August 2007
Published 21 September 2007
Online at stacks.iop.org/JPhysCM/19/406227

Abstract

Motivated by evidences of helical wrapping of polymeric molecules around nanotubes, we perform a systematic study of how the electronic density of states of nanotubes is affected by the introduction of a coiling polarizing potential. The coiling perturbation, characterized by the wrapping angle, the polarizing width and the polarization strength, introduces an additional geometrical chirality that may not necessarily coincide with the intrinsic chiral angle of the nanotube. Features of the electronic density of states are shown to depend on this perturbation with different degrees of sensitivity. When correlated with the binding energy between the nanotube and the wrapping molecule, we find that noticeable changes in the density of states occur only for minimally bound structures.

(Some figures in this article are in colour only in the electronic version)

Carbon nanotubes are low-dimensional nanoscopic structures with remarkable physical properties. More than a decade of intensive research on carbon nanotubes gives support to the general belief that these are outstanding materials with tremendous potential for technological applications. As regards their intrinsic physical properties, among the most interesting are that they are mechanically very strong, are excellent conductors of thermal energy, and may be metallic or semiconducting depending exclusively on the spatial arrangement of their atomic structure. This latter property results from certain geometrical conditions that determine whether or not a nanotube can display extended electronic states at its Fermi level.

Doping is the typical way of changing the electronic properties of any given material. In fact, by adding impurities to a host material one can change its transport characteristics. Typically, impurities are spatially uncorrelated and are responsible for multiply scattering the electrons that travel across the structure. As a result of this scattering, the transmitted wavefunctions are reduced and so is the overall conductance of the material. This is the case, for instance, in conductance modulation of nanotubes through both atomic and molecular

doping [1–3]. To give a concrete example, the ability to change the conductance of a nanotube exposed to certain gaseous molecules is driving the research to build sensitive nanodevices capable of detecting minute concentrations of specific substances [4].

Of a very different nature, geometrically ordered doping agents can also affect the conductivity of a host material but examples are not as plentiful and common as their disordered counterparts. Having nanotubes as hosts, the list of examples in which impurities are spatially ordered is even more limited. Although the underlying lattice remains the same, in this case the spatially ordered perturbing potential that acts on the nanotube due to the impurities may follow a different geometrical arrangement. Depending on the strength of the perturbation as well as on its spatial geometry, this can in principle lead to interference effects, both constructive and destructive, that will affect the overall band structure of the material. Rather than a purely abstract and speculative hypothesis, here we argue that this may actually occur with nanotubes helically wrapped by linear charge distributions.

Charged one-dimensional-like structures such as polymers and DNA molecules are known to interact with nanotubes and to produce unusual physical properties: the former affecting the mechanical [5], thermal [6, 7] and electronic [8] properties of nanotube–polymer composite materials and the latter being used as a technique to separate nanotubes of different types [9]. As a result of this interaction, these molecules can sometimes coat the walls of a nanotube. Regarding the coating morphology, there are evidences indicating that these long molecules tend to wrap around the tubular structures in a helical fashion [10, 11]. Because the presence of a charge distribution near the tube is expected to polarize the local electronic density in its proximity, the effect of the wrapping can be reproduced by the introduction of a helically symmetric potential. While not necessarily completely geometrically ordered, this potential is certainly not random either. Despite previous suggestions that the helicity displayed by the wrapping molecules should follow the intrinsic chirality of the nanotube [12], contrary arguments suggest that these bulky molecules are not capable of resolving the atomic structure of the underlying lattice [13, 14]. In this case tubes may then be exposed to two different helical pitches, namely, the intrinsic chirality of the nanotube and that associated with the wrapping potential. It is our goal here to investigate the effect that this combination of chiralities may have on the nanotube band structure and, in particular, on its electronic density of states (DOS).

Nanotubes are here described by the following effective tight-binding Hamiltonian

$$\hat{H}_0 = \sum_{j,j'} |j\rangle \gamma \langle j'|, \tag{1}$$

where $|j\rangle$ represents the π-orbital centred at atom j, $|j'\rangle$ is a nearest-neighbour orbital centred on atom j', and γ is the nearest-neighbour electronic hopping, hereafter chosen to be our energy unit. Such a simple Hamiltonian is known to reproduce well the electronic structure of nanotubes. The presence of the linear charge distribution will be accounted for by assuming that it can polarize what lies in its close proximity. In this case, these polarizable entities are the carbon atoms on the tube which are subjected to the following perturbing potential

$$\hat{V} = \sum_{\ell} |\ell\rangle \lambda \langle \ell|. \tag{2}$$

In the equation above, the index ℓ labels the carbon atoms affected by the proximity to the wrapping molecules and λ represents the corresponding shift in their on-site potential as a result of the induced polarization. This latter parameter can in principle be determined in accordance with the measured binding energy between the nanotube and its wrapping molecules, thus reflecting the intuitive notion that strong binding between the parts should induce a substantial degree of polarization on the tube. Furthermore, the fact that ionic doping agents can affect the amount of charge carried on the DNA backbone suggests that we may consider a range of values for λ, which we will hereafter regard as an adjustable parameter.

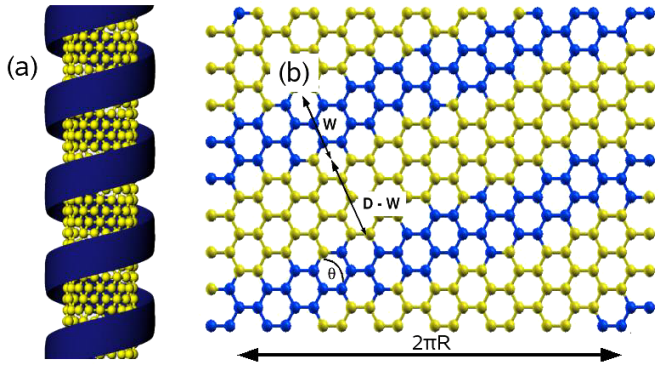

Figure 1. Schematic representation of a helically-wrapped nanotube. In (a) we display a polymeric molecule represented by a continuous charge distribution of width W coiling at an angle θ around the surface of the nanotube. In (b) we display the corresponding geometry in the unwrapped representation. The atoms to be perturbed are indicated by the dark (blue) balls, while the unperturbed atoms are the light (yellow) balls. D is defined in the picture as the distance between equivalent atoms of neighbouring stripes. Also depicted is the circumference of the nanotube ($2\pi R$) where R is the nanotube radius.

Figure 1 shows a possible configuration in which a polymeric molecule is helically wrapped around a nanotube. As previously mentioned, it is unlikely that the wrapping molecules are able to resolve the atomic structure of the underlying nanotube. Therefore, rather than considering the precise atomic structure of the molecules, we treat them as a continuous charge distribution of uniform width wrapped around the nanotube at an angle θ, as depicted in the unwrapped scheme by the two-dimensional stripe in figure 1(b). The lateral dimension of the wrapping molecule determines the width W of this stripe. We assume that the induced polarization represented by the perturbing potential in equation (2) affects all carbon atoms immediately below the charged stripe. With these simplifications in place, we can map the problem of helical charge distributions surrounding the surface of a nanotube by introducing a helically-symmetric square well potential that follows a similar chirality. In principle, the angle θ bears no direct relation to the chiral angle α of the underlying nanotube.

The perturbation $\hat{V}$ is characterized by the wrapping angle θ, the strength λ, and the width W. To assess how the electronic structure of a nanotube is influenced by the wrapping potential, we have performed a systematic study of how the electronic DOS is affected as some of these different parameters are varied. In particular, since they are quasi-one-dimensional, nanotubes have densities of states containing several van Hove singularities (VHS). By locating these singularities and tracking how they evolve as the aforementioned parameters are varied, one can view, at least from a qualitative point of view, how nanotubes respond to such perturbations.

The sequence adopted in this paper is as follows: in section 1, we discuss the details of our calculations, as well as defining some useful concepts; in sections 3–5, we present results for the dependence of a few physical observables on the microstructure parameters λ, θ and W; and in section 6 we present conclusions and discussion.

1. Calculational details

For the calculation of electronic energy levels of any given structure, it is often convenient to use suitable coordinate systems that reflect the symmetry of the problem under investigation. In this case one would expect the introduction of a helical coordinate system to solve the

single-particle Schroedinger equation. However, this can be avoided if we treat the system in its unwrapped form, as shown in figure 1(b). Bearing in mind the periodic boundary conditions required to represent the true cylindrical shape of the tube, we can visualize the helical potential as an array of equally-spaced stripes of finite width on a boundless graphene sheet.

To calculate the electronic structure of the system in the nearest-neighbour tight-binding model, we directly solve the Schroedinger equation in reciprocal space, which requires the introduction of a repeating unit cell. We assume that the perturbing potential makes P full twists in the space of Q primitive unit cells of the nanotube, and that P and Q are integers with no common factor. Then if $\vec{T}$ is the translational vector of the nanotube's unit cell, the perturbed structure is periodic along the tube axis (chosen as our z-axis), with period $Q|\vec{T}|$. As a concrete example, the system depicted in figure 1(b) has $P = 2$, $Q = 9$, and $\vec{T} = a\hat{z}$, where a is the distance between two crystallographically equivalent atoms in a graphene lattice, and $\hat{z}$ is a unit vector along the tube axis.

Since we have a periodic system, we can apply the Bloch theorem to write $\hat{H} = \sum_k \hat{H}_k$, where k is the wavenumber in reciprocal space. If there are N electronic states in this supercell, for each value of $k \in [0, \frac{2\pi}{Q|\vec{T}|})$ we must diagonalize the matrix $\langle l|\hat{H}_k|m\rangle$ to obtain the N eigenvalues ω_{jk}. To construct the density of states per atom, $\rho(E)$, we use the eigenvalue representation for the single-particle Green function

$$\rho(E) = \frac{-Q|\vec{T}|}{2\pi^2}\mathrm{Im}\left(\int_0^{\frac{2\pi}{Q|\vec{T}|}} \mathrm{d}k \sum_{j=1}^{N} \frac{1}{(E + \mathrm{i}\eta) - \omega_{jk}}\right), \tag{3}$$

where η is a real quantity that should be taken in the limit of $\eta \to 0$.

Once we have the DOS per atom, we can calculate auxiliary quantities such as the Fermi level of the composite material, determined by demanding that

$$\int_{-\infty}^{E_\mathrm{F}} \rho(E) = 1 + \Delta C. \tag{4}$$

This last follows from the observation that there should be one p_z electron per carbon atom plus any contribution coming from a possible charge transfer ΔC between the nanotube and the perturbing agent.

Of particular interest to us is the behaviour of the DOS. In the case of semiconducting nanotubes in the absence of any perturbations, the DOS is characterized by an energy gap separating a series of VHS. For perturbation-free metallic tubes, the same singularities are separated by a finite dispersionless region around E_F. It turns out that in the case of metallic nanotubes, the DOS acquires gaps when subjected to perturbations of various types, one primary example being the introduction of weak curvature effects [15]. In the case considered here, the introduction of a helical perturbation is no different and always induces the opening of small gaps at the Fermi level. As we shall see, under certain circumstances this gap is so small that it is unlikely that its effect would ever be observable, being easily washed out by thermal effects and/or by small charge transfers between the parts. Nevertheless, it is important to quantify them so that we can estimate characteristic temperatures and/or critical levels of charge transfer required to perceive a possible metal–insulator transition. Bearing in mind our goal of investigating how the characterizing features of the electronic DOS of nanotubes are affected by the helical perturbation, we look at how these gaps are affected by the potential $\hat{V}$. More specifically, we determine how the VHS (and indirectly the associated gaps) change with the variation of three independent parameters: θ, the angle which the stripe makes with the tube axis, W, the width of the perturbation and λ, which governs the amplitude of the perturbation.

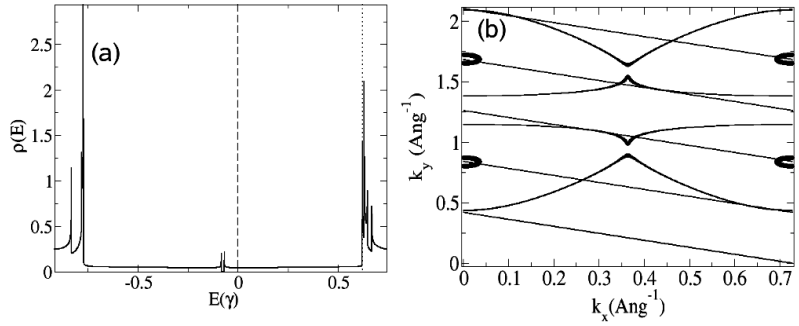

Figure 2. (a) The DOS for a (4, 4) armchair nanotube perturbed at an angle of $\theta = \frac{\pi}{3}$ rad by a 2.0 Å wide stripe of amplitude $\lambda = -0.3\gamma$. The dashed line corresponds to the on-site energy of the unperturbed nanotube, while the dotted line marks the maximum of the first VHS above the Fermi level. (b) The corresponding energy iso-surfaces in reciprocal space for a graphene sheet perturbed by a series of equally spaced stripes. The straight lines depict the quantized wavevectors that are permitted due to the boundary conditions. Two distinct iso-energy surfaces are presented, corresponding to the two energies highlighted in (a). The iso-surface corresponding to the VHS energy is seen to touch the lines of quantization tangentially, in contrast to that of the lower energy.

2. Location of van Hove singularities

It is well known that the VHS associated with a SWNT have a simple geometric interpretation. The Brillouin zone of graphene corresponds to a hexagon in reciprocal space, and the effect of wrapping a graphene sheet into a nanotube confines the electronic wavefunction in the circumferential direction. This leads to a quantization of the circumferential component of the wavevector. Accordingly, the electronic structure of the resulting nanotube is obtained by considering only those states which lie in a series of discrete equally spaced lines overlaid on the Brillouin zone of graphene. If one plots the iso-energy surfaces for the graphene sheet for different energies, one sees that the VHS in the DOS of the nanotube correspond precisely to those energies where the allowed wavevector lines touch the iso-energy surfaces tangentially.

One can apply the same reasoning in the case of our perturbed system. In this case, however, the Brillouin zone will be contained in a parallelogram, due to the oblique shape of our real space unit cell. Again, the spatial confinement of the electronic wavefunctions induces a wavevector quantization. Unsurprisingly, the VHS of the composed system can be tracked in the same fashion as in the case of the unperturbed system, as the points of tangency of these quantized lines to the iso-energy surfaces appropriate to the perturbed system. It is worth stressing that the constant-energy surfaces are no longer determined by the electronic structure of a simple graphene sheet. In this case, it corresponds to the electronic states associated with a sheet of hexagonally ordered atoms whose on-site potentials display the striped geometry depicted in figure 1(b). This is illustrated in figure 2. On the left panel (a), we plot the DOS of a (4, 4) nanotube perturbed by a helical potential defined by $\theta = \pi/3$ rad, $W = 2.0$ Å and $\lambda = -0.3\gamma$. Two vertical dashed lines are also included, one at $E = 0.0$ and another at $E = 0.63\gamma$. The former (thick line) marks the on-site energy of the unperturbed carbon atoms and the latter (thin line) coincides with a VHS displayed in the DOS. The right panel (b) shows the corresponding constant-energy plots in reciprocal space superimposed with equally spaced lines representing the allowed wavevectors that the electronic states can have. Once again the thick-line iso-surface corresponds to $E = 0$ whereas the thin-line curves are associated with $E = 0.63\gamma$. It is evident that, for $E = 0$, the iso-surface intersects (non-tangentially) the quantized wavevector lines indicating the existence of extended electronic

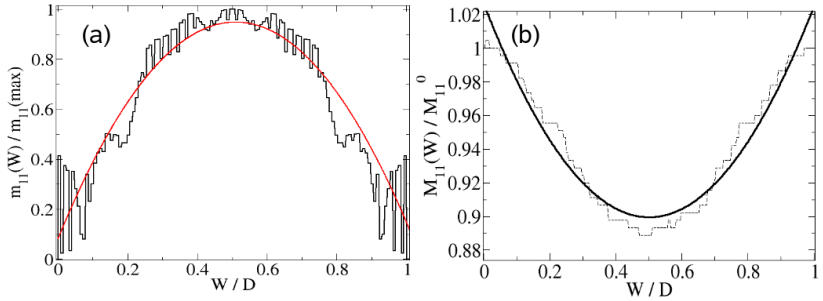

Figure 3. (a) Dependence of the minigap m_{11} on the width W for an (18, 0) nanotube coiled by a uniform stripe at angle $\theta = 0.978$ rad and $\lambda = -0.3\gamma$. The maximum value of m_{11} occurs at $W/D = 0.5$ and is used here as a reference. The smooth solid line is a quadratic fitting. The overall trend is of a non-monotonic increase in the perturbation-induced minigap. (b) Dependence of the transition M_{11} on the width W for the (18, 0) nanotube (dashed, black curve) together with a quadratic regression (continuous curve) in units of the unperturbed transition $M_{11}^0 = 0.57\gamma$. $\lambda = -0.3\gamma$ in all cases. The overall trend is towards a red-shifting of the transition, with a energy change of at most about 11%.

states at that energy, also confirmed by the finiteness of its DOS. In contrast, for $E = 0.63\gamma$, the thick-line iso-surface tangentially intersects the quantized lines, proving that the geometrical interpretation mentioned above is also valid for the nanotube in the presence of the helical perturbation. With such a simple geometrical picture, one can easily trace how the VHS positions are affected by the helical potential. Bearing in mind that optical transitions are usually dependent on the distance between neighbouring VHS, this picture seems useful to study how the electronic structure of a nanotube is affected by the wrapping perturbation. In what follows we adopt the standard notation of $M_{j,j}$ and $S_{j,j}$ for the separation between the jth VHS for metallic and semiconducting tubes, respectively. Following a similar notation, we represent the perturbation-induced minigaps in metallic tubes by the quantity m_{11}.

3. *W*-dependence

The effect of the helical potential on the nanotube atoms can be separated into two disjoint contiguous subsets: a stripe of polarized atoms, and another in which the atoms are unperturbed. W is an upper bound for the perpendicular distance between any two perturbed atoms, as measured normal to the direction of the perturbation. Following figure 1(b), we define D as the distance between two equivalent atoms of neighbouring stripes. It follows from these definitions that W must range between 0 and D. It is worth noting that stripe widths such that $W/D \approx 0$ (low coverage) are somewhat equivalent to the cases of nearly full coverage in which $W/D \approx 1$. In each of these limiting cases, we expect the shape of the DOS to approach that of the uniform tube, albeit in the second case with a rigid shift of its centre of mass from $E_F = 0$ to the value $E_F = \lambda$. Despite the fact that W can take any value in the range $[0, D]$, the dependence of the quantities of interest as a function of W must acquire a step-like quality. This is because for any value W, there is a minimum quantity ΔW that the stripe must be widened by in order to contain a new perturbed atom. This is illustrated in figure 3(a) where we show how m_{11} depends on W for an (18, 0) nanotube with $\lambda = -0.3\gamma$ and $\theta = 0.978$ rad. Plotted in units of m_{11} for $W/D = 0.5$, which is the maximum value for the minigap ($m_{11} = 0.0056\gamma$), we see that the minigap scales approximately quadratically with the ratio W/D. The locations of the main VHS are also affected by the perturbation. In this case, the energy distance between the first VHS on either side of the Fermi level, here labelled M_{11}

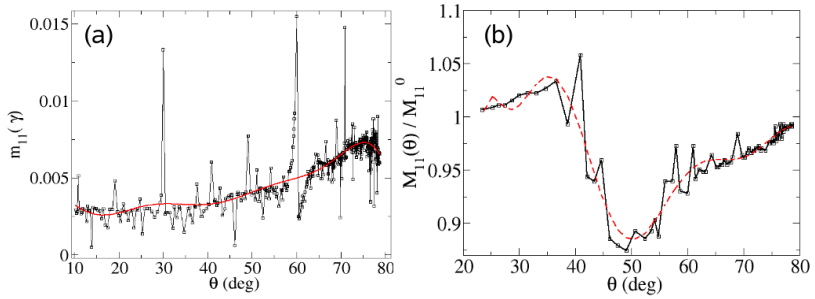

Figure 4. (a) A plot of m_{11}, for various coiling angles (full line, with points). This plot is in units of γ. (b) A plot of the energy difference between the two VHS on either side of the Fermi level for an (18, 0) zigzag nanotube (corresponding to the M_{11} transition in the pure tube) for different coiling angles. The plot is normalized to the size of the transition for the clean tube M_{11}^0. The amplitude of the perturbation is held constant at -0.3γ, and so is the width of the perturbation at $W = 6.7$ Å. The smooth lines corresponds to a high order polynomial approximation to the curve, and are intended as a guide to the eye.

by analogy with the unperturbed tube, is plotted in figure 3(b) as a function of the width W for the same set of parameters, in units of the unperturbed transition energy M_{11}^0. Once again the step-like behaviour of the calculated results are smoothened by fitting the curve to a quadratic regression to the data points. The overall trend is towards a red-shifting of the transition, with a maximum change of approximately 11%. The duality between the unperturbed and the perturbed atoms is highlighted by the degree to which the curve is symmetric about the point $W/D = 0.5$.

4. θ-dependence

An interesting question to ask is what is the qualitative behaviour of the quantities of interest when the angle θ is varied. In our scheme, the coiling angle is given by the formula

$$\theta = \arctan\left(\frac{P|\vec{C}|}{Q|\vec{T}|}\right), \tag{5}$$

where $\vec{C}$ is the chiral vector of the tube. While it is conceivable that the perturbation could follow a truly incommensurate configuration ($\frac{P}{Q}$ irrational), it is also clear that the coiling angle appropriate to that system will lie arbitrarily close to that of a commensurate system, provided we allow P and Q to be sufficiently large. Since we must have a periodic system, θ cannot be varied continuously, but must increase in discrete steps, similarly to the width-dependence results presented above. We have investigated the angular dependence of these quantities for an (18, 0) zigzag nanotube. Such a tube is an ideal candidate for these investigations since the fundamental unit cell is only $\frac{2a}{\sqrt{3}}$ in length, but $18a$ in width, where a is the lattice parameter of the graphene structure. This allows one to consider a wide range of angles. Holding both the width of the stripe $W = 6.7$ Å and the amplitude of the perturbation $\lambda = -0.3\gamma$ constant, figure 4 shows both m_{11} and M_{11} transitions as a function of the coiling angle. Panel (a) displays m_{11} in units of γ for various coiling angles and panel (b) does the same for M_{11} in which it is expressed in units of the unperturbed transition M_{11}^0. Each graph has a smoother curve acting as a guide to the eye which reflects the overall trend of the above quantities and how they depend on the coiling angle. What is evident from panel (a) is that the stepwise fluctuations that surround the smooth curve becomes much more pronounced at values of θ corresponding

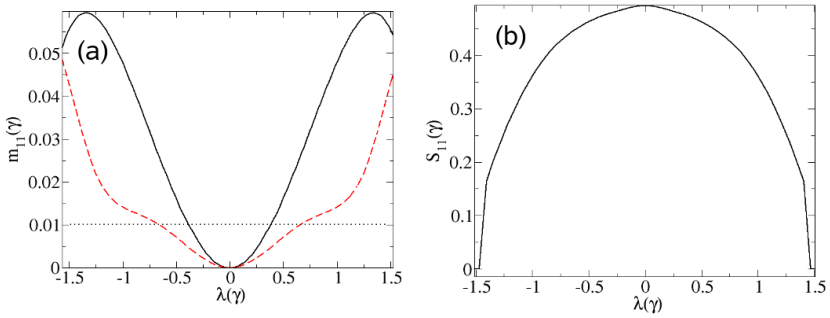

Figure 5. (a) A plot of the size of the minigap m_{11} as a function of the polarization strength parameter λ for two different chiralities and coiling angles. The solid (black) curve corresponds to a (6, 6) nanotube perturbed by a stripe at an angle of 64.3°, while the dashed (red) curve corresponds to a (6, 0) nanotube subject to a stripe at an angle of 34.7°. The dotted line indicates where the minigap energy is equivalent to room temperature. In (b) we plot the fundamental semiconducting transition as it depends on the perturbation amplitude for a (7, 0) nanotube wrapped by a stripe at angle 39.0°. A monotonic red-shifting of the gap is observed in the range of interest. In all cases the width of the perturbation is 5.33 Å.

to coiling angles that are perfectly commensurate with the high symmetry directions of the nanotube. In those cases the perturbation-induced minigaps can be as large as 40 meV. As far as the M_{11} transition is concerned, one can clearly see in panel (b) that at low coiling angles there is a noticeable blue-shifting of the transition, whereas at mid to high coiling angles there is a decrease in the transition energy. Such a non-monotonic behaviour in the angle-dependent electronic structure has been reported for the case of helical short-range potentials in cylindrical geometries [14].

5. λ-dependence

Intuitively, one expects that the features of the DOS investigated here will vary continuously as a function of the parameter λ, in contrast to the discontinuous behaviour found as a function of W and of θ. This would mean that the VHS separations should vary continuously as a function of the perturbation amplitude. As depicted in figure 5, we indeed find that they depend continuously on the amplitude of the perturbation λ. In the case of the (6, 0) zigzag and (6, 6) armchair nanotubes which are metallic in the absence of a perturbation, we find that for small perturbation amplitudes, the minigaps grow monotonically as we increase the magnitude of the perturbation. In contrast, for the semiconducting (7, 0) tube, we see the opposite trend in S_{11}. In this case, the gap decreases as a function of λ. This shows that as we increase the strength of the helical perturbations, metallic tubes are driven into becoming more semiconducting-like whereas the originally semiconducting tubes have the opposite effect of reducing their gaps.

The systematic study carried out above shows how the DOS may respond to a coiling perturbation that represents the effect of helically wrapping molecules surrounding a nanotube. Two characteristic features of the DOS were investigated, namely the perturbation-induced minigaps m_{11} as well as those associated with the transitions M_{11} and S_{11}. They were shown to depend on the characteristic features of the perturbing potential such as the wrapping angle θ, the polarizing width W and the strength of the polarizing potential λ. More than a purely academic exercise, this is a valuable point to assess how some physical quantities may respond to the presence of a wrapping charge distribution. For the sake of illustration, rather than treating λ as a free parameter, it is instructive to estimate its value by equating the

perturbation-induced change in total energy to the measured binding energy between the wrapping molecules and nanotubes. While the polarization interaction is certainly not the only component of the measured binding energy, under the assumption that other contributions such as the elastic energy and the van der Waals interaction are small, it will be the dominant contribution. This allows us to estimate how strongly bound the parts must be before any perceptible change occurs in the DOS. Following figure 5(a), absent any charge transfer, we find that to open a gap comparable to room temperature requires a value of λ of about 1 eV in the case of a wrapped (6, 6) nanotube, and that larger minigaps require monotonically larger λ. For the case of organic polymers [16], we find the magnitude of λ to be too small to produce a minigap of this magnitude. Likewise, for the case of undoped DNA molecules [17] it is also not sufficiently strong to produce significant alterations in their electronic structure features. These examples seem too weakly bound to produce dramatic changes in the electronic structure of the host nanotube. This suggests that extra charge must be required on the backbone of the wrapping molecule to increase its polarizing effect and, in turn, its binding energy. In fact, ionic doping has been reported to affect the optical response of DNA–nanotube composites [18] by increasing the amount of charge on the DNA backbone, which seems consistent with our findings.

6. Conclusions

In summary, we have performed a systematic study of the effect of a coiling polarizing potential on the electronic structure of carbon nanotubes. The perturbation characterized by the wrapping angle θ, the polarizing width W and the polarization strength λ introduces an additional geometrical chirality that may not necessarily coincide with the intrinsic chiral angle of the nanotube. It is noted that the largest changes however occur in the commensurate case. Features of the electronic density of states characterizing the VHS transitions were seen to depend on θ, W and λ with different degrees of sensitivity. Furthermore, a geometrical representation similar to the one used for pure nanotubes was used to trace how the VHS evolved with changes of the perturbation parameters. Furthermore, we estimate a minimum binding energy between the tube and the wrapping molecules to generate a minigap comparable in size to the ambient thermal energy. We find that while it is in principle possible to alter the electronic structure of nanotubes by wrapping a charge distribution around them, noticeable changes tend to occur for the cases in which the binding energy molecules are more strongly bound to the nanotubes. We argue that changes in the optical response induced by ionic doping on DNA–nanotube composites may be one such example.

Acknowledgments

MSF acknowledges the financial support of Science Foundation Ireland. AW acknowledges support received from the Irish Research Council for Science, Engineering and Technology under the EMBARK initiative. The authors wish to acknowledge the SFI/HEA Irish Centre for High-End Computing (ICHEC) for the provision of computational facilities and support.

References

[1] Latil S, Roche S and Charlier J C 2005 Electronic transport in carbon nanotubes with random coverage of physisorbed molecules *Nano Lett.* **5** 2216–9

[2] Latil S, Roche S, Mayou D and Charlier J C 2004 Mesoscopic transport in chemically doped carbon nanotubes *Phys. Rev. Lett.* **92** (25)

[3] Adessi Ch, Roche S and Blase X 2006 Reduced backscattering in potassium-doped nanotubes: *ab initio* and semiempirical simulations *Phys. Rev.* B **73** (12)
[4] An K H, Jeong S Y, Hwang H R and Lee Y H 2004 Enhanced sensitivity of a gas sensor incorporating single-walled carbon nanotube–polypyrrole nanocomposites *Adv. Mater.* **16** 1005–9
[5] Dalton A B, Collins S, Munoz E, Razal J M, Ebron Von H, Ferraris J P, Coleman J N, Kim B G and Baughman R H 2003 Super-tough carbon-nanotube fibres *Nature* **423** 703
[6] Berber S, Kwon Y-K and Tomanek D 2000 Unusually high thermal conductivity of carbon nanotubes *Phys. Rev. Lett.* **84** 4613–6
[7] Kim P, Shi L, Majumdar A and McEuen P L 2001 Thermal transport measurements of individual multiwalled nanotubes *Phys. Rev. Lett.* **87** 215502
[8] Biercuk M J, Llaguno M C, Radosavljevic M, Hyun J K, Johnson A T and Fischer J E 2002 Carbon nanotube composites for thermal management *Appl. Phys. Lett.* **80** 2767–9
[9] Zheng M, Jagota A, Semke E D, Diner B A, Mclean R S, Lustig S R, Richardson R E and Tassi N G 2003 DNA-assisted dispersion and separation of carbon nanotubes *Nat. Mater.* **2** 338–42
[10] McCarthy B, Coleman J N, Curran S A, Dalton A B, Davey A P, Konya Z, Fonseca A, Nagy J B and Blau W J 2000 Observation of site selective binding in a polymer nanotube composite *J. Mater. Sci. Lett.* **19** 2239–41
[11] O'Connell M J, Boul P, Ericson L M, Huffman C, Wang Y, Haroz E, Kuper C, Tour J, Ausman K D and Smalley R E 2001 Reversible water-solubilization of single-walled carbon nanotubes by polymer wrapping *Chem. Phys. Lett.* **342** 265–71
[12] Czerw R, Guo Z, Ajayan P M, Sun Y P and Carroll D L 2001 Organization of polymers onto carbon nanotubes: a route to nanoscale assembly *Nano Lett.* **1** 423–7
[13] Coleman J N and Ferreira M S 2004 Geometric constraints in the growth of nanotube–templated polymer monolayers *Appl. Phys. Lett.* **84** 798–800
[14] Wall A and Ferreira M S 2006 Electronic contribution to the energetics of helically wrapped nanotubes *Phys. Rev.* B **74** (23)
[15] Glseren O, Yildirim T and Ciraci S 2002 Systematic *ab initio* study of curvature effects in carbon nanotubes *Phys. Rev.* B **65** 153405
[16] Coleman J N, Fleming A, Maier S, O'Flaherty S, Minett A I, Ferreira M S, Hutzler S and Blau W J 2004 Binding kinetics and swnt bundle dissociation in low concentration polymer–nanotube dispersions *J. Phys. Chem.* B **108** 3446–50
[17] Coleman J N 2007 private communication
[18] Heller D A, Jeng E S, Yeung T-K, Martinez B M, Moll A E, Gastala J B and Strano M S 2006 Optical detection of DNA conformational polymorphism on single-walled carbon nanotubes *Science* **311** 508–11